Applied Radiation and Isotopes xxx (xxxx) xxx–xxx

Contents lists available at ScienceDirect

Applied Radiation and Isotopes

journal homepage: www.elsevier.com/locate/apradiso

SUMCOR: Cascade summing correction for volumetric sources applying MCNP6

M.S. Dias*, R. Semmler, D.S. Moreira, M.O. de Menezes, L.F. Barros, R.V. Ribeiro, M.F. Koskinas

Instituto de Pesquisas Energéticas e Nucleares, IPEN-CNEN/SP, Av. Prof. Lineu Prestes 2242, 05508-000 São Paulo, SP, Brazil

HIGHLIGHTS

- Code SUMCOR developed for cascade summing correction is described.
- MCNP6 is used to track individual points inside the volumetric source.
- Cascade summing correction is based on the matrix formalism.
- Results are compared with two intercomparisons organized by the ICRM-GSWG.

ARTICLE INFO

Keywords:
Cascade summing
Monte Carlo
Gamma-ray emission
HPGe
MCNP6

ABSTRACT

The main features of code SUMCOR developed for cascade summing correction for volumetric sources are described. MCNP6 is used to track histories starting from individual points inside the volumetric source, for each set of cascade transitions from the radionuclide. Total and FEP efficiencies are calculated for all gamma-rays and X-rays involved in the cascade. Cascade summing correction is based on the matrix formalism developed by Semkow et al. (1990). Results are presented applying the experimental data sent to the participants of two intercomparisons organized by the ICRM-GSWG and coordinated by Dr. Marie-Cristine Lépy from the Laboratoire National Henri Becquerel (LNE-LNHB), CEA, in 2008 and 2010, respectively and compared to the other participants in the intercomparisons.

1. Introduction

There is a continuing effort inside the ICRM (International Committee for Radionuclide Metrology) community to improve the codes for calculating cascade summing corrections, for samples of different geometries and decay scheme characteristics. Reports on comparisons were presented at the 2009, 2011, 2013 and 2015 ICRM meetings, showing the evolution of the codes.

Following this effort, the Nuclear Metrology Laboratory (LMN - Laboratório de Metrologia Nuclear), in São Paulo, developed a code for cascade summing correction for volumetric sources called SUMCOR. The present paper describes the main features of this code and the results obtained with data supplied by Dr. Marie-Cristine Lépy from the Laboratoire National Henri Becquerel (LNE-LNHB), CEA. These data were sent to the participants of two intercomparisons, which are described in Lépy et al. (2010, 2012).

2. Methodology

2.1. Monte Carlo simulation

Code MCNP6 (Goorley et al., 2013) was used for all simulations. Fig. 1 shows the model used for simulation of point sources at different distances from the detector window, as depicted by code VISED (Carter and Schwarz, 2005). In this picture the source was located at 2 cm. All detailed geometric aspects and materials described in reference Lépy et al. (2010), including the radiographs, were considered.

It was noticed that the presence of the PPMA (poly(methyl methacrylate)) holder around the source gives rise to a pronounced scattering in the calculated spectrum, mainly at intermediate gamma-ray energies (around 400–700 keV) where the Compton Effect is dominant. As a consequence, the total detection efficiency is larger when compared to the value calculated without the PPMA holder.

For volume sources, two source-detector models were created: the first (called Model 1) describes all aspects of the source and detector systems, and the source location is defined at a random point sampled

* Correspondence to: Instituto de Pesquisas Energéticas e Nucleares, IPEN-CNEN/SP, Centro do Reator de Pesquisas – CRPq, C.P. 11049, Pinheiros, 05422-970 São Paulo, SP, Brazil.
E-mail address: msdias@ipen.br (M.S. Dias).

http://dx.doi.org/10.1016/j.apradiso.2017.09.014
Received 9 March 2017; Received in revised form 4 September 2017; Accepted 10 September 2017

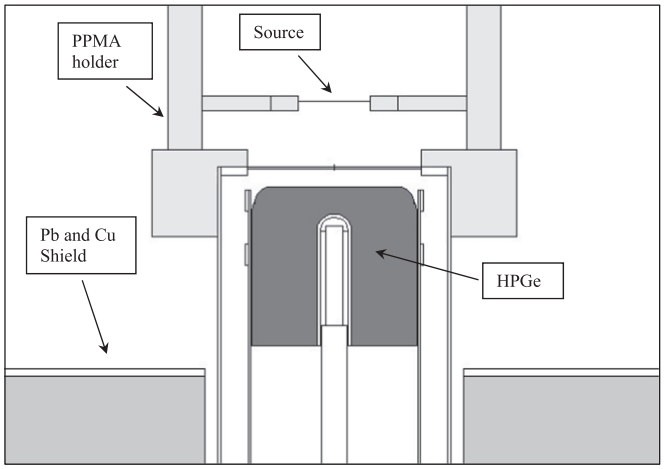

Fig. 1. Partial view of the source-Detector Model 1 for MCNP6 as drawn by code VISED (Carter and Schwarz, 2005). For volume sources, the PPMA holder has been replaced by the radioactive solution container.

inside the source volume; the second (called Model 2) is identical to Model 1 except the source location which is defined to cover all the source volume. In both models, the PPMA holder used for point sources has been replaced by the containers and contact materials (Mylar, PPMA and copper) used in the intercomparison for volume sources, as described in reference Lépy et al. (2012).

Using Model 1, for each point location, 10^5 histories were followed for each gamma-ray or X-ray present in the cascades and a total of 50 points were sampled from a uniform distribution inside the source volume. For the volumetric source, applying Model 2, 10^6 histories were followed for each gamma-ray or X-ray present in the cascades. More histories were followed for Model 2 because the calculation was performed only once, whereas for Model 1 it was performed fifty times for different points inside the source volume.

2.2. Cascade summing correction

This correction was calculated applying the matrix formalism described by Semkow et al. (1990) which are the results shown in the tables. Additional calculations were performed using Menno Blaauw's equations (Blaauw and Gelsema, 2003) but the running time using turned out to be much longer, when compared to the matrix formalism. The summing correction factors calculated by these two formalisms were in good agreement with each other. For the LS-Ratio calculations, the matrix formalism was modified in order to follow the prescription given by Blaauw and Gelsema (2003).

The summing correction factor was calculated as the weighted average value from all individual points inside the source volume. The weighting factor was the corresponding FEP (full energy absorption peak efficiency - ε_p) of the corresponding transition in the cascade, as follows:

$$\overline{F_S} = \frac{\sum_{i=1}^{N_p} F_{S\,i}\,\varepsilon_{p\,i}}{\sum_{i=1}^{N_p} \varepsilon_{p\,i}} \quad (1)$$

Where:

N_P	is the total number of random points inside the source volume;
ε_{pi}	is the full energy absorption peak (FEP) efficiency for each random point, for the corresponding transition in the cascade;
F_Si	is the summing correction factor for each random point, for the corresponding transition in the cascade;

Points closer to the detector have higher peak efficiencies; therefore the weighted mean obtained by Eq. (1) corresponds to a larger correction when compared to the simple mean. This can be considered the best estimate to the summing correction factor included in the tables.

All relevant decay data for the radionuclides involved were taken from NUCLEIDE (Vanin et al., 2004; Bé et al., 2013). They are: energy levels; transition probabilities; total and K shell conversion coefficients; X-ray fluorescence yields and metastable half-lives. These data were input and stored in the code corresponding arrays.

For the case of electron capture decay nuclides, the K X-rays were included but the contribution from other shells was not considered. For beta minus decay the contribution from electrons were not considered as well. A future improvement to SUMCOR is planned to include L X-rays and beta ray contributions. For beta plus decay and volume sources, the present version of SUMCOR may be used by adding the corresponding annihilation quanta to the corresponding positron decay levels in the decay scheme. This is possible because the annihilation process occurs near the positron decay location. For point sources, the present version of SUMCOR code is not suitable because the annihilation process may occur outside the source location, changing the 511 keV annihilation photon detection efficiency.

2.3. SUMCOR calculation procedure

Fig. 2 is a block diagram showing the main features of code SUMCOR. In this figure, the following parameters are defined:

NP	is the number of random points inside the source volume;
NT	is the number of transitions in the cascade;
FEPP	is the full energy absorption peak (FEP) efficiency for each random point, for each energy in the cascade;
TEFP	is the total efficiency for each random point, for each energy in the cascade;
FSUMP	is the cascade summing correction factor for each random point, for each energy in the cascade;
LSRATIO	is the Linear to Square Ratio for each random point, for each energy in the cascade;
FEPV	is the full energy absorption peak efficiency for the volume source (Model 2);
TEFV	is the total efficiency for the volume source (Model 2);
FSUMV	is the cascade summing correction factor for the volume source (Model 2).

The running process follows several steps. Initially, the source-detector system Model 1 is selected in MCNP6 and a random point is sampled inside the volumetric source. For each X-ray or gamma-ray energy present in the input data, the total and FEP efficiencies are calculated for that point by MCNP6 and the results for all transitions are stored. Then the cascade summing correction factor is calculated for that point, considering all cascades.

Subsequently, a new random point is sampled and this process is repeated until the last point is sampled ($i = NP$). The weighted average summing correction factors and their standard deviations are calculated, considering all sampled points inside the source and all gamma-transitions in the cascades. These are the results shown in all the tables of the present work, applying Eq. (1). At this stage, the average total and FEP efficiencies are calculated, as well as the LS-Ratio described by Blaauw and Gelsema (2003), considering all sampled points.

Next, the source-detector system Model 2 is selected for the MCNP6 code and the total and FEP efficiencies are calculated for the volumetric source, for all transitions. Then the cascade summing correction factor is calculated for all cascades, following the same formalism applied previously, but only once considering the volumetric source efficiencies. The cascade summing correction is calculated using the total and FEP efficiencies for Model 2 taken from the output of MCNP6 for all transitions. This procedure is biased because it considers simple average

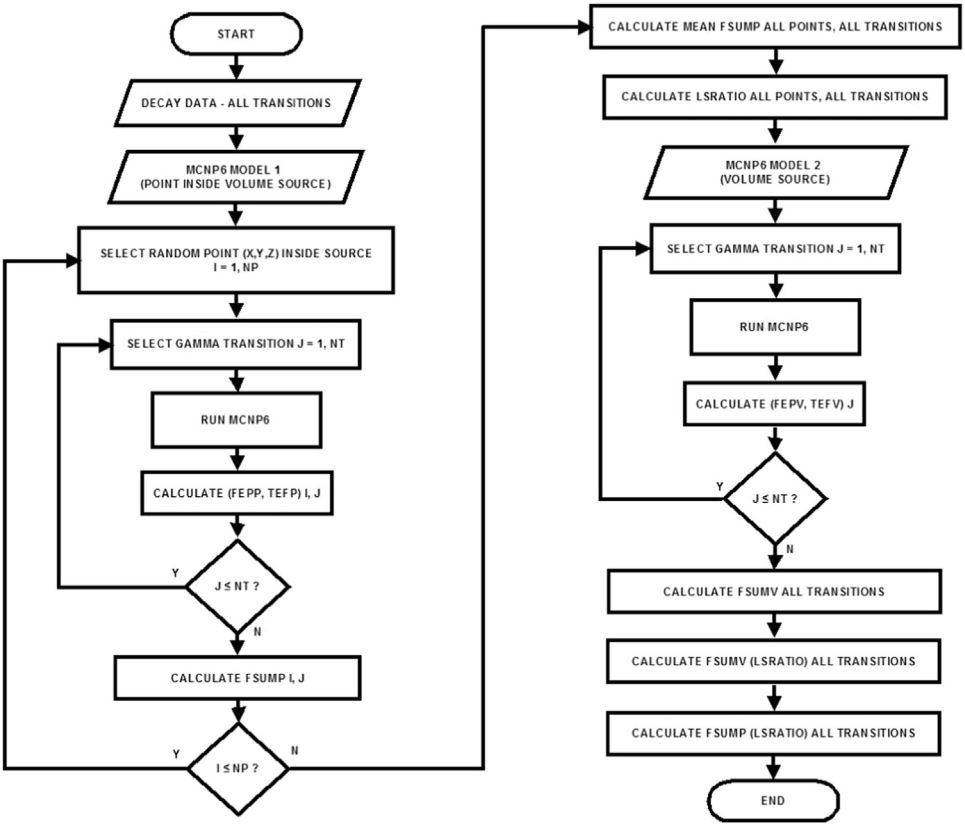

Fig. 2. Block diagram showing the main features of code SUMCOR. The parameters are described in the text.

of cascade summing correction for all sampled points. This result is also included in the tables for volumetric sources.

Finally, the cascade summing correction was calculated by applying the LS-Ratio to the average efficiencies obtained with the volumetric source (Model 2). These results are presented in the tables for comparison. The metastable cases may be considered by applying the equations described in the literature (Sima and Arnold, 2008). This latter feature was not included in the results for the present work but is planned for a future publication. The present paper is focused on the data supplied to participants in two previous intercomparisons described in Lépy et al. (2010, 2012). They were analyzed by code SUMCOR and the results compared to the average values from the other participants for the case of point sources, and to the experimental results for the case of volumetric sources.

MCNP6 was processed with *multi-core* in *mode p* using the default parameters and libraries; *mode p e* was tried but it resulted in a too long processing time and was disregarded for SUMCOR processing. The total and peak efficiencies were calculated at 121, 867 and 1408 keV for a point source located 10 cm away from the crystal, in both *modes*: *p* and *p e*, running 3×10^8 histories. The percent differences between the two modes at these three energies were respectively: 0.01%, −1.9% and −2.3%, for peak efficiencies, and 0.01%, + 1.1% and + 2.2%, for total efficiencies. Therefore it only partially explains the observed difference between the MCNP and the experimental results, indicating that other objects not included in the model may explain the differences.

Although the full energy peak efficiency may be biased if electron transport in the detector is neglected, the average agreement around 4.0% with experimental values was considered satisfactory. Inaccuracies in the calculated total efficiency were corrected on basis of experimental values as described in the following section. The CPU was an *i5 4570* with 3.2 GHz. The processing time depended heavily on the radionuclide due to the number of transitions in the decay scheme. The longest time was observed for the ^{152}Eu capture branch which lasted 16,000 s. This value corresponds to 90 transitions (including electron capture branches), 50 points inside the source volume and 10^5 histories per point for each transition.

2.4. Estimation of uncertainty

For the radionuclides presented here: ^{152}Eu and ^{134}Cs, the uncertainties in the cascade summing correction associated with the decay scheme parameters, taken from NUCLEIDE (Vanin et al., 2004; Bé et al., 2013), were estimated and are presented in Table 5. The uncertainty propagation recommended by the GUM (JCGM, 2008) is difficult to implement; for this reason the propagation of distributions was applied and incorporated into code SUMCOR. The procedure described in the reference Sima and Lépy (2016) has been adopted and applied to Semkow matrix formalism. The decay scheme parameters were sampled from a normal distribution with best estimates and standard uncertainties given by the tabulated values from NUCLEIDE (Vanin et al., 2004; Bé et al., 2013). The parameters considered were: gamma-ray emission probabilities, total and K conversion coefficients. From the first two of these parameters the gamma-ray transition probabilities were calculated. Next, all branching ratios were calculated with appropriate balancing from the highest level. Finally, the P_K and ω_K parameters were sampled. Therefore, all the steps described in section 5 of reference Sima and Lépy (2016) were followed. For each sampling a new decay scheme is computed, taking into account all appropriate correlations. As a result, the uncertainty due to all decay parameters is calculated. The uncertainty due to the efficiencies was calculated separately, as described in the following sections.

The main source of uncertainty comes from the values of total and FEP efficiencies calculated by MCNP6. This uncertainty was estimated by comparing the calculated efficiency with the fittings to experimental data sent to the participants of the first intercomparison (Lépy et al., 2010), which were obtained with point sources located 10 cm away from the detector window. From this comparison it was observed a difference around 4.0% in the calculated FEP efficiency and an

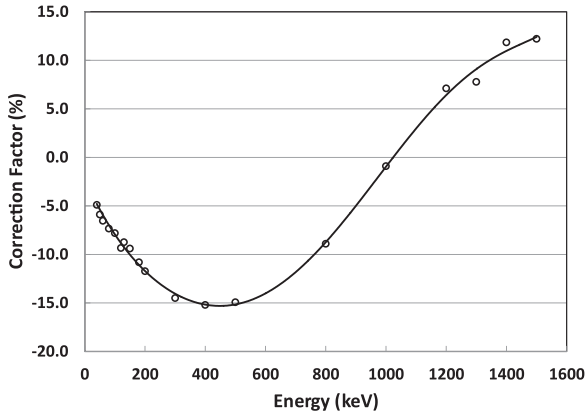

Fig. 3. Correction factor applied to the total efficiency calculated by MCNP6 (in percent).

underestimation of the total efficiency by the simulation in the range 1–15% below 1000 keV and an overestimation in the range 1–10% above 1000 keV. These differences between experiment and simulation may be attributable to imperfections in modelling or improper account for surrounding scattering.

In order to keep the simulation results free from any correction factor taken from the experiment, these differences may be treated as uncertainties in the summing correction factor. However, the summing correction results will be systematically biased because the calculated total efficiency is different from the experiment. A second alternative is to apply a correction factor to the calculated total efficiency in order to approximate it to the experimental value. In the present work, this procedure was performed by comparing the MCNP6 results to the fittings applied to experimental data described in reference Lépy et al. (2010) and obtained with point sources positioned 10 cm away from the detector window. The percent differences between the calculated and experimental values are shown in Fig. 3. The minimum around 500 keV may be due to extra scattering in neighbor objects around the HPGe detector not included in the modelling; the increase at high energies may be due to improper modelling of the internal crystal hole. A polynomial fitting was applied to these points and this function was incorporated into SUMCOR, in order to correct the calculated total efficiency.

It was observed that the ratio between the calculated and experimental total efficiencies remains approximately constant as the distance from source to detector window moves from 2 cm to 10 cm. Therefore, it was possible to apply the same correction factor for different distances. An uncertainty of ± 10% was attributed to the corrected total efficiency, which was the value estimated for the original experimental fitting (Lépy et al., 2010).

The correction factor indicated by Fig. 3 and applied to point sources was also applied to volumetric sources, and proved suitable for correcting extra scattering not predicted by MCNP6 modelling by comparing SUMCOR results with experiment. However, a better estimate would be to compare the calculated volumetric total efficiencies with experimental ones obtained with monoenergetic radionuclides, which is planned for future work.

The procedure for uncertainty propagation applied to the decay scheme parameters was also applied to obtain the uncertainty due to the total and peak efficiencies. The values were sampled from a normal distribution with best estimates given by the MCNP6 calculation and with standard uncertainties of 4% for peak efficiencies and 10% for total efficiencies, respectively. For the case of total efficiency, the best estimate included the polynomial correction factor.

Whenever one of the parameters: decay scheme or efficiencies was sampled, the other remained fixed to the best estimate value, in order to obtain the two individual uncertainty components shown in Table 5. In order to avoid efficiency variation from point to point inside the volume, the source position was kept at the center of the source volume during the parameter sampling. The estimated uncertainty was properly normalized to account for the difference between the summing correction factor for the point source and for the volumetric source.

In the case of volume sources, an additional spreading in the summing correction factor appears caused by the variation in the efficiencies, due to changes in solid angle and attenuation between the sampled point inside the source volume and the HPGe detector. Code SUMCOR is able to calculate both the variance in the efficiencies and in the summing correction factor. This is possible because these parameters are calculated individually for each sampled point. As a result, the uncertainty due to this effect can be calculated with accuracy. The uncertainty in the average summing correction factor is reduced as the number of sampled points inside the source volume is increased. For the case of $\boldsymbol{n}$ sampled points, the reduction is by a factor of $\sqrt{n}$. Therefore, the uncertainty included in the total value was due to the *finite number* of sampled points. If this number goes to infinity this uncertainty goes to zero, but in order to keep a reasonable processing time, the number of sampled points was restricted to 50 per source. This uncertainty corresponds to the one obtained by repeating the run several times with the same number of points per group and considering the standard deviation of the distribution.

The total error presented in Table 5 corresponds to the sum in quadrature, considering these three uncertainty components as independent: finite number of points inside the source volume, decay scheme parameters and detector efficiency. For point sources, the first component is zero.

A measure of agreement between SUMCOR and the Intercomparison results was introduced in the tables: the $\boldsymbol{Z}$ score, which is defined as:

$$Z = \frac{F_S - F_I}{\sqrt{\sigma_s{}^2 + \sigma_I{}^2}} \tag{2}$$

Where:

- $\boldsymbol{F_S}$ is the summing correction calculated by code SUMCOR (Model 1), using Eq. (1);
- $\boldsymbol{F_I}$ is the summing correction simple mean value from other codes, or the experimental result presented in the Intercomparison;
- $\boldsymbol{\sigma_S}$ is the standard deviation in the summing correction calculated by code SUMCOR;
- $\boldsymbol{\sigma_I}$ is the standard deviation in the simple mean value from other codes, or in the experimental result presented in the Intercomparison.

Acceptable values should be within $-\boldsymbol{2} \leq \boldsymbol{Z} \leq \boldsymbol{2}$ for 95% confidence interval.

3. Results and discussion

Initially, the summing correction results from code SUMCOR were compared to the group of participants of the intercomparison with point sources described in reference Lépy et al. (2010). The summing correction results obtained at the energies of ^{152}Eu, calculated at 2, 5 and 10 cm away from the HPGe window, are presented in Table 1. A good agreement with the simple mean values of the intercomparison (ICRM_GSWG, 2009) can be observed in all cases, within the estimated uncertainties and the Z score values showed a small positive bias, but resulted well within the acceptable limits.

Table 1 includes the strongly discrepant points in the intercomparison. The values reported later (Lépy et al., 2010) at the energy 122 keV from ^{152}Eu, in which the strongly discrepant points were excluded, resulted at 2, 5 and 10 cm respectively: 1.173(28), 1.057(9) and 1.020(2), in even better agreement with SUMCOR code results, which were: 1.194(19), 1.061(3) and 1.021(2).

The summing correction factor for the EC transitions are heavily

Table 1
Summing correction results for point sources obtained at the energies of ^{152}Eu at different distances from the HPGe detector window. The numbers between parentheses correspond to the standard deviation in the last digits. The intercomparison Mean Value was taken from the literature (ICRM_GSWG, 2009).

Distance	2 cm			5 cm			10 cm		
Energy (keV)	SUMCOR	Comparison Mean Value	Z	SUMCOR	Comparison Mean Value	Z	SUMCOR	Comparison Mean Value	Z
121.8	1.194(19)	1.157(49)	0.70	1.061(3)	1.051(15)	0.66	1.021(2)	1.021(14)	0.01
244.7	1.307(33)	1.245(71)	0.79	1.092(10)	1.074(19)	0.82	1.030(3)	1.030(17)	0.00
344.3	1.060(7)	1.061(11)	−0.09	1.021(2)	1.021(3)	0.12	1.008(1)	1.008(2)	0.18
411.1	1.166(20)	1.164(31)	0.06	1.055(8)	1.054(9)	0.12	1.020(2)	1.021(5)	−0.14
444.0	1.259(26)	1.227(84)	0.36	1.078(9)	1.071(22)	0.30	1.025(3)	1.028(16)	−0.19
564.0	1.241(25)	1.240(136)	0.01	1.072(8)	1.075(37)	−0.07	1.023(2)	1.030(25)	−0.29
688.6	1.205(30)	1.152(71)	0.69	1.060(10)	1.048(23)	0.46	1.018(3)	1.019(19)	−0.03
778.9	1.102(18)	1.096(22)	0.20	1.036(7)	1.034(6)	0.16	1.014(2)	1.011(8)	0.40
867.4	1.370(38)	1.301(81)	0.78	1.108(13)	1.092(25)	0.58	1.035(3)	1.035(19)	−0.02
964.1	1.247(30)	1.180(62)	0.98	1.079(10)	1.055(18)	1.18	1.031(3)	1.024(19)	0.35
1085.8	1.056(18)	1.012(42)	0.96	1.023(8)	1.004(13)	1.29	1.013(2)	1.006(10)	0.70
1089.7	1.086(17)	1.086(19)	0.01	1.029(8)	1.029(5)	0.01	1.011(2)	1.010(7)	0.09
1112.1	1.203(29)	1.148(59)	0.84	1.060(10)	1.044(17)	0.81	1.020(3)	1.018(13)	0.13
1212.9	1.359(37)	1.284(78)	0.87	1.105(12)	1.086(20)	0.80	1.033(3)	1.032(11)	0.10
1299.1	1.103(18)	1.099(19)	0.15	1.037(7)	1.034(7)	0.26	1.015(2)	1.013(5)	0.41
1408.0	1.214(28)	1.155(59)	0.90	1.063(10)	1.049(16)	0.73	1.019(3)	1.018(13)	0.06

dependent on the summing-out with K X-rays coming from the capture process. For instance, comparing SUMCOR results at 122 keV, with and without capture X-rays contribution, it was estimated that 57% of the correction comes from capture X-rays. Therefore, the accurate estimate of this contribution is very important.

The summing correction results for point sources obtained at the energies of ^{134}Cs are presented in Table 2. This radionuclide is a beta-gamma emitter; therefore there is no contribution from capture X-rays to the cascade summing correction. A good agreement can be observed in all cases, within the estimated uncertainties and the *Z* score values resulted small and well within the acceptable limits.

The summing correction results for volumetric sources correspond to Volume 2 described in reference Lépy et al. (2012) and are presented in Tables 3 and 4. Several codes which took part in that comparison may have their performance improved since that time; therefore the results shown in the cited reference may not correspond to the present status of the codes. This is more critical for volumetric sources because the summing correction factor changes from point to point inside the source and a proper account of this effect must be considered. For this reason it was decided to compare the SUMCOR results directly to the reported experimental values, except for the case of ^{134}Cs with Mylar as contact, for which experimental results were not reported in the cited reference Lépy et al. (2012). In this case the SUMCOR results were compared to the mean of the results from other participants (CMV Comparison Mean Value).

The SUMCOR results at the energies of ^{152}Eu are presented in Table 3, for the chosen contact materials. The first column corresponds to the weighted average given by Eq. (1). In principle, this may be considered the best estimate of the correction calculated by the code. A good agreement with experimental results can be observed in most cases, within the estimated uncertainties and the *Z* score values resulted within acceptable limits and with no appreciable bias. This may indicate that the correction applied to the total efficiency was satisfactory. The contribution from K X-rays is expected to be smaller when compared to point sources due to the long path to cross the radioactive solution and the container wall.

The second column corresponds to the LS-Ratio estimate, using Model 2 for calculation of efficiencies. The results are in close agreement with those obtained by Eq. (1) for most cases, indicating the convenience of this approximation. The third column corresponds to the cascade summing correction calculated by using Model 2. In general, it can be observed a negative bias showing lower corrections than expected.

The summing correction results for volume sources obtained at the energies of ^{134}Cs are presented in Table 4. Eq. (1), LS-Ratio and Model 2 are shown in a similar way as in Table 3. For Eq. (1), a good agreement with experimental results can be observed in most cases, within the estimated uncertainties and the *Z* score values resulted within the acceptable limits. The LS-Ratio results are in good agreement with Eq. (1). As expected, Model 2 shows a negative bias when compared to Eq. (1).

The main components of the cascade summing uncertainty are shown in Table 5. The first column (s1) corresponds to the statistical fluctuation due to finite number of sampled points; the second column (s2) to the uncertainty in the decay scheme parameters and (s3)

Table 2
Summing correction results for point sources obtained at the energies of ^{134}Cs at different distances from the HPGe detector window. The numbers between parentheses correspond to the standard deviation in the last digits. The intercomparison Mean Value was taken from the literature (ICRM_GSWG, 2009).

Distance	2 cm			5 cm			10 cm		
Energy (keV)	SUMCOR	Comparison Mean Value	Z	SUMCOR	Comparison Mean Value	Z	SUMCOR	Comparison Mean Value	Z
242.8	1.173(23)	1.165(46)	0.15	1.058(6)	1.056(16)	0.12	1.021(2)	1.020(6)	0.17
326.5	1.227(23)	1.216(60)	0.17	1.076(5)	1.079(28)	−0.12	1.028(2)	1.027(3)	0.20
475.3	1.164(23)	1.165(29)	−0.02	1.056(4)	1.059(21)	−0.16	1.020(2)	1.020(3)	0.07
563.2	1.173(23)	1.173(30)	0.00	1.057(5)	1.058(10)	−0.11	1.019(2)	1.021(3)	−0.42
569.3	1.172(24)	1.171(29)	0.04	1.058(6)	1.059(9)	−0.09	1.021(2)	1.022(4)	−0.17
604.7	1.098(14)	1.098(15)	0.00	1.034(4)	1.036(5)	−0.35	1.012(1)	1.013(3)	−0.17
795.8	1.106(20)	1.103(18)	0.11	1.036(4)	1.037(5)	−0.08	1.014(2)	1.014(4)	−0.11
801.9	1.164(23)	1.160(29)	0.10	1.056(4)	1.055(9)	0.05	1.020(2)	1.020(3)	0.11
1038.6	1.033(18)	1.031(15)	0.10	1.011(5)	1.012(8)	−0.13	1.005(2)	1.005(4)	0.07
1167.9	0.917(19)	0.922(19)	−0.19	0.968(8)	0.968(12)	0.03	0.989(3)	0.988(4)	0.29
1365.2	0.868(24)	0.875(25)	−0.20	0.955(10)	0.948(6)	0.61	0.984(4)	0.981(5)	0.46

Table 3
Summing correction results for volume sources obtained at the energies of ^{152}Eu with different contacts above the detector window. The numbers between parentheses correspond to the standard deviation in the last digits. The intercomparison experimental values correspond to Volume 2 and were taken from reference Lépy et al. (2012). The *Z* score is defined according to Eq. (2).

Contact	Mylar					PPMA					Copper				
Energy (keV)	EXP	SUMCOR Model 1 Eq. (1)	Z	SUMCOR Model 2 LS-Ratio	SUMCOR Model 2	EXP	SUMCOR Model 1 Eq. (1)	Z	SUMCOR Model 2 LS-Ratio	SUMCOR Model 2	EXP	SUMCOR Model 1 Eq. (1)	Z	SUMCOR Model 2 LS-Ratio	SUMCOR Model 2
121.8	1.216(11)	1.206(21)	−0.43	1.173	1.167	1.193(11)	1.188(21)	−0.19	1.166	1.149	1.082(11)	1.085(8)	0.24	1.068	1.073
244.7	1.346(17)	1.308(34)	−1.01	1.321	1.259	1.260(16)	1.285(29)	0.75	1.368	1.229	1.135(15)	1.120(11)	−0.81	1.124	1.104
344.3	1.101(11)	1.066(6)	−2.86	1.078	1.060	1.078(12)	1.066(6)	−0.93	1.335	1.056	1.078(12)	1.065(6)	−0.94	1.070	1.056
411.1	1.197(18)	1.177(17)	−0.81	1.212	1.162	1.169(18)	1.178(17)	0.35	1.155	1.151	1.170(19)	1.172(18)	0.09	1.182	1.148
444.0	1.264(21)	1.191(21)	−2.44	1.276	1.210	1.235(20)	1.227(24)	−0.27	1.193	1.185	1.112(19)	1.096(9)	−0.74	1.113	1.085
564.0	1.289(41)	1.239(25)	−1.05	1.277	1.206	1.225(39)	1.222(24)	−0.07	1.190	1.182	1.138(37)	1.096(9)	−1.12	1.115	1.084
688.6	1.262(67)	1.169(23)	−1.31	1.233	1.169	1.253(68)	1.182(22)	−1.00	1.145	1.146	0.983(45)	1.035(4)	1.15	1.054	1.031
778.9	1.089(17)	1.108(14)	0.88	1.146	1.100	1.096(18)	1.108(14)	0.54	1.093	1.093	1.085(17)	1.105(14)	0.91	1.126	1.091
867.4	1.343(33)	1.356(37)	0.26	1.426	1.309	1.310(33)	1.332(32)	0.48	1.274	1.274	1.135(27)	1.148(13)	0.45	1.179	1.129
964.1	1.224(24)	1.229(27)	0.14	1.281	1.202	1.179(21)	1.215(24)	1.13	1.179	1.176	1.038(21)	1.062(6)	1.11	1.086	1.056
1085.8	1.061(25)	1.059(13)	−0.09	1.093	1.054	1.046(20)	1.056(14)	0.42	1.038	1.045	0.951(23)	0.985(3)	1.48	1.006	0.989
1089.7	1.130(29)	1.094(14)	−1.12	1.136	1.087	1.060(24)	1.094(13)	1.25	1.079	1.081	1.027(27)	1.092(14)	2.14	1.117	1.080
1112.1	1.183(28)	1.187(25)	0.11	1.237	1.165	1.155(22)	1.175(22)	0.65	1.175	1.175	0.994(24)	1.030(4)	1.50	1.054	1.027
1212.9	1.331(61)	1.344(36)	0.18	1.420	1.300	1.194(48)	1.320(31)	2.21	1.140	1.142	1.083(46)	1.143(13)	1.26	1.173	1.125
1299.1	1.139(39)	1.109(14)	−0.73	1.157	1.101	1.035(30)	1.109(14)	2.24	1.094	1.094	1.024(35)	1.105(14)	2.16	1.133	1.092
1408.0	1.204(31)	1.194(25)	−0.26	1.252	1.171	1.151(21)	1.180(22)	0.97	1.147	1.147	1.004(26)	1.036(4)	1.23	1.065	1.032

Table 4
Summing correction results for volume sources obtained at the energies of ^{134}Cs with different contacts above the detector window. The numbers between parentheses correspond to the standard deviation in the last digits. The intercomparison experimental values correspond to Volume 2 and were taken from reference Lépy et al. (2012). The *Z* score is defined according to Eq. (2). For Mylar contact, the comparison is made with the mean value from the other codes (CMV – Comparison Mean Value).

Contact	Mylar					PPMA					Copper				
Energy (keV)	CMV	SUMCOR Model 1 Eq. (1)	Z	SUMCOR Model 2 LS-Ratio	SUMCOR Model 2	EXP	SUMCOR Model 1 Eq. (1)	Z	SUMCOR Model 2 LS-Ratio	SUMCOR Model 2	EXP	SUMCOR Model 1 Eq. (1)	Z	SUMCOR Model 2 LS-Ratio	SUMCOR Model 2
475.3	1.164(27)	1.171(16)	0.24	1.182	1.163	1.142(39)	1.175(16)	0.77	1.176	1.152	1.242(49)	1.195(18)	−0.91	1.186	1.152
563.2	1.180(27)	1.182(15)	0.05	1.188	1.173	1.192(16)	1.185(16)	−0.33	1.188	1.161	1.182(18)	1.207(17)	0.98	1.204	1.161
569.3	1.181(27)	1.181(18)	0.01	1.196	1.172	1.197(14)	1.184(18)	−0.56	1.188	1.161	1.177(16)	1.206(20)	1.13	1.204	1.161
604.7	1.104(15)	1.104(10)	−0.02	1.112	1.099	1.122(12)	1.105(10)	−1.06	1.107	1.093	1.117(14)	1.117(11)	0.02	1.118	1.093
795.8	1.106(15)	1.110(12)	0.23	1.120	1.105	1.108(16)	1.112(12)	0.21	1.116	1.098	1.099(16)	1.125(13)	1.23	1.131	1.098
801.9	1.166(25)	1.170(16)	0.14	1.186	1.162	1.158(19)	1.173(16)	0.59	1.179	1.152	1.152(19)	1.192(18)	1.52	1.200	1.151
1038.6	1.038(9)	1.047(10)	0.63	1.053	1.044	1.090(41)	1.047(10)	−1.01	1.051	1.042	1.095(44)	1.056(12)	−0.85	1.069	1.045
1167.9	0.934(16)	0.943(11)	0.49	0.942	0.945	0.909(24)	0.943(11)	1.28	0.946	0.951	0.923(29)	0.948(10)	0.80	0.964	0.959
1365.2	0.883(19)	0.907(14)	1.02	0.902	0.907	0.899(19)	0.908(14)	0.37	0.908	0.914	0.865(25)	0.913(13)	1.68	0.924	0.925

Table 5
Uncertainty components of the summing correction factor (in absolute values). The first column (s1) corresponds to the statistical fluctuation due to finite number of sampled points; the second column (s2) corresponds to the decay scheme parameters; the third column (s3) corresponds to the total and peak efficiencies, sampled independently and considered together. These partial uncertainties were added in quadrature in order to give the overall uncertainty (sT).

Contact - PPMA									
Eu-152					Cs-134				
Energy (keV)	S1	S2	S3	ST	Energy (keV)	S1	S2	S3	ST
121.8	0.012	0.0058	0.015	0.021	475.3	0.010	0.0007	0.013	0.016
244.7	0.020	0.0050	0.020	0.029	563.2	0.011	0.0017	0.011	0.016
344.3	0.003	0.0025	0.005	0.006	569.3	0.010	0.0007	0.014	0.018
411.1	0.008	0.0029	0.015	0.017	604.7	0.006	0.0006	0.009	0.010
444.0	0.016	0.0055	0.017	0.024	795.8	0.006	0.0006	0.010	0.012
564.0	0.016	0.0055	0.017	0.024	801.9	0.010	0.0007	0.013	0.016
688.6	0.014	0.0056	0.016	0.022	1038.6	0.002	0.0008	0.010	0.010
778.9	0.005	0.0026	0.012	0.014	1167.9	0.004	0.0014	0.011	0.011
867.4	0.025	0.0050	0.020	0.032	1365.2	0.005	0.0006	0.013	0.014
964.1	0.016	0.0048	0.017	0.024					
1085.8	0.004	0.0060	0.012	0.014					
1089.7	0.004	0.0026	0.012	0.013					
1112.1	0.014	0.0046	0.016	0.022					
1212.9	0.024	0.0048	0.020	0.031					
1299.1	0.005	0.0026	0.013	0.014					
1408.0	0.014	0.0044	0.016	0.022					

corresponds to the total and peak efficiencies, sampled independently and considered together. The main contributions to the total uncertainty (sT) come from the efficiencies and, to a lesser extent, from the finite number of sampled points. The contributions from the decay scheme parameters are smaller.

The overall uncertainty was in general around 10% of the correction and, in some cases, lower than the experimental uncertainty. This result together with a Z score within the expected range for most cases was considered satisfactory. A few cases where $|Z|$ resulted larger than two will be object of further investigation. Further refinements in MCNP6 modelling, including more scattering objects around the HPGe detector, may reduce this uncertainty.

4. Conclusion

The calculation of cascade summing corrections for point and volumetric sources was succeeded based on MCNP6 modelling and complemented by experimental data, to achieve an uncertainty around 10% of the correction. Further refinements in modelling may reduce this uncertainty.

Agreement with the mean values from the first intercomparison (Lépy et al., 2010) and with the experimental results from the second intercomparison (Lépy et al., 2012) were achieved for most cases, considering both point and volumetric sources of ^{152}Eu and ^{134}Cs, within the estimated uncertainties.

Future work is foreseen to include other comparisons between the present method and the *L-S Ratio* method (Blaauw and Gelsema, 2003), applying the efficiencies for volumetric sources calculated by SUMCOR to the *L-S* formalism, as well as validation for metastable nuclides (Sima and Arnold, 2008). The uncertainty calculation for the *L-S* formalism applying SUMCOR code is also planned.

Acknowledgements

The authors are very grateful to Dr. Marie-Cristine Lépy from the Laboratoire National Henri Becquerel (LNE-LNHB, CEA) for providing the data sent to the participants of the intercomparisons described in references (Lépy et al., 2010) and (Lépy et al., 2012), and to the Brazilian National Council for Scientific and Technological Development (CNPq) for partial support to the present research project (Grant number 302747/2014-1). The authors are also grateful to Dr. Maurício Moralles from IPEN for the valuable discussions.

References

Bé, M.-.M., Chisté, V., Dulieu, C., Mougeot, X., Chechev, V.P., Kondev, F.G., Nichols, A.L., Huang, X., Wang, B., 2013. Table of Radionuclides, Monographie BIPM-5. Bureau International des Poids et Mesures, Pavillon de Breteuil, F-92310 Sèvres, France. ⟨http://www.nucleide.org/DDEP_WG/DDEPdata.htm⟩.

Blaauw, M., Gelsema, S.J., 2003. Cascade summing in gamma-ray spectrometry in marinelli-beaker geometries: The third efficiency curve. Nucl. Instrum. Methods Phys. Res. Sect. A: Accel. Spectrom. Detect. Assoc. Equip. 505, 311–315.

Carter, L.L., Schwarz, R.A., 2005. MCNP Visual Editor Computer Code Manual. MCNP, Richland, WA.

Goorley, JohnT., James, MichaelR., Booth, ThomasE., Brown, ForrestB., Bull, JeffreyS., Cox, LawrenceJ., Durkee, JoeW. Jr., Elson, JayS., Fensin, MichaelLorne, Forster, RobertA. III, Hendricks, JohnS., Hughes, H.Grady. III, Johns, RussellC., Ki, A.J., 2013. Initial MCNP6 Release Overview - MCNP6 version 1.0 - LA-UR-13-22934.

ICRM_GSWG, 2009. Report on the meeting of the Gamma Spectrometry Working Group [WWW Document]. ICRM_GSWG_Report_2009. URL ⟨http://www.nucleide.org/ICRM_GSWG/ICRM_GSWG_Report_2009.doc⟩.

JCGM, 2008. JCGM 101: 2008 Evaluation of measurement data — Supplement 1 to the Guide to the expression of uncertainty in measurement — Propagation of distributions using a Monte Carlo method.

Lépy, M.-C., Altzitzoglou, T., Anagnostakis, M.J., Arnold, D., Capogni, M., Ceccatelli, A., De Felice, P., Dersch, R., Dryak, P., Fazio, A., Ferreux, L., Guardati, M., Han, J.B., Hurtado, S., Karfopoulos, K.L., Klemola, S., Kovar, P., Lee, K.B., Ocone, R., Ott, O., Sima, O., Sudar, S., Švec, A., Van Tao, C., Thanh, T.T., Vidmar, T., 2010. Intercomparison of methods for coincidence summing corrections in gamma-ray spectrometry. Appl. Radiat. Isot. 68, 1407–1412.

Lépy, M.C., Altzitzoglou, T., Anagnostakis, M.J., Capogni, M., Ceccatelli, A., De Felice, P., Djurasevic, M., Dryak, P., Fazio, A., Ferreux, L., Giampaoli, A., Han, J.B., Hurtado, S., Kandic, A., Kanisch, G., Karfopoulos, K.L., Klemola, S., Kovar, P., Laubenstein, M., Lee, J.H., Lee, J.M., Lee, K.B., Pierre, S., Carvalhal, G., Sima, O., Van Tao, C., Thien Thanh, T., Vidmar, T., Vukanac, I., Yang, M.J., 2012. Intercomparison of methods for coincidence summing corrections in gamma-ray spectrometry-part II (volume sources). Appl. Radiat. Isot. 70, 2112–2118.

Semkow, T.M., Mehmood, G., Parekh, P.P., Virgil, M., 1990. Coincidence summing in gamma-ray spectroscopy. Nucl. Instrum. Methods Phys. Res. Sect. A Accel. Spectrom. Detect. Assoc. Equip. 290, 437–444.

Sima, O., Arnold, D., 2008. A tool for processing decay scheme data that encompasses coincidence summing calculations. Appl. Radiat. Isot. 66, 705–710.

Sima, O., Lépy, M.C., 2016. Application of GUM Supplement 1 to uncertainty of Monte Carlo computed efficiency in gamma-ray spectrometry. Appl. Radiat. Isot. 109, 493–499.

Vanin, V.R., Castro, R.M., Browne, E., 2004. Table of Radionuclides, Monographie BIPM-5. Bureau International des Poids et Mesures, Pavillon de Breteuil, F-92310 Sèvres, France. ⟨http://www.nucleide.org/DDEP_WG/DDEPdata.htm⟩.